1 **Factors driving metal partition in ionic liquid-based acidic aqueous biphasic**

2 **systems**

3

4 Ana R. F. Carreira,[a] Helena Passos,[a]* Nicolas Schaeffer,[a] Lenka Svecova,[b] Nicolas

5 Papaiconomou,[c] Isabelle Billard,[b] and João A. P. Coutinho[a]

6

7 [a] CICECO - Aveiro Institute of Materials, Department of Chemistry, University of Aveiro, 3810-

8 193 Aveiro, Portugal

9 [b] Univ. Grenoble Alpes, Univ. Savoie Mont Blanc, CNRS, Grenoble INP (Institute of Engineering

10 and Management Univ. Grenoble Alpes), LEPMI, 38000 Grenoble, France

11 [c] Université Côte d'Azur, CNRS, Institut de Chimie de Nice, UMR 7272, 06108 Nice, France.

12

13 *Corresponding author. Email: hpassos@ua.pt

Abstract

The factors influencing metal partition in acidic aqueous biphasic systems (AcABS) containing phosphonium-based ILs are still poorly explored. To assess their influence the effect of the IL counter anion, acid and its concentration, and temperature, were systematically evaluated on the extraction of four transition metals (Cu(II), Co(II), Ni(II), and Mn(II)) and the lanthanide Ce(IV). The AcABS based on HCl showed good ability to extract Co(II) and Cu(II) to the IL-rich phase. In contrast, AcABS based on H_2SO_4 showed overall poor metal extraction, except for the $[P_{44414}]Cl$ + H_2SO_4 + H_2O system. The latter showed good Cu(II) affinity at higher H_2SO_4 concentrations. The biphasic systems based on HNO_3 were unable to extract transition metals to the IL-rich phase, with chloride from $[P_{444414}]Cl$ hampering Ce(IV) extraction. The $[P_{444414}]Cl$ + H_2SO_4 + H_2O system was further optimized by adding small amounts of HCl to the system. The extraction efficiency of the metals is linked to the charge density of the metal-complex and its inherent free energy of hydration, the anion/water molar ratio changes induced by temperature and ionic strength, and the dissociation degree of the acid. By using these parameters it was possible to tune the selectivity and efficiency of the AcABS. Moreover, metal extraction was found to preferentially occur via an ion-pair mechanism, with split anion extraction taking place in AcABS containing different anions.

Keywords:

1. Introduction

Solvent extraction is a widely used separation technique based on the distribution of a target molecule between two immiscible phases.[1] Conventional metal liquid-liquid extraction systems often rely on non-ecofriendly volatile organic diluents to overcome the viscosity of extractants. Ionic liquids (ILs) were identified as a possible solution to this issue.[2] ILs are an alternative class of solvents composed of a large organic cation and an organic or inorganic anion. When carefully designed they have negligible vapor pressure, high solvation capacity, good chemical stability and low-flammability. [2][3] Hydrophobic ionic liquids (ILs) were proposed as a good option for metal extraction since they can simultaneously act as metal extractants and diluents.[4] Although liquid-liquid extraction systems based on hydrophobic ILs are a potential upgrade from the conventional solvent extractions systems, they still pose some issues. The structural requirements to achieve hydrophobic ILs constrain their chemical diversity. Moreover, the viscosity and toxicity of such ILs raise concerns[5,6] It is important to highlight that due to their ionic nature even "hydrophobic" ILs are hygroscopic and can incorporate significant amounts of water, especially when converted to mole fraction.[7] In the context of this work, we assign the term hydrophobic to designate ILs that present limited aqueous solubility whilst hydrophilic ILs are fully miscible with water across all binary compositions.

The disadvantages of hydrophobic ILs are fueling the transition from liquid-liquid extraction systems based on hydrophobic ILs to hydrophilic ones when applicable. The use of hydrophilic ILs for the formation of aqueous biphasic systems (ABS) is versatile, allowing the use of a larger variety of more benign ILs, and applicable to metal extraction.[8–10] Overall ABS are seen as more biocompatible liquid-liquid extraction systems due to water being the main component of their two-phases.[11] In the formation of a ternary ABS, a hydrophilic IL is combined with water and a salting-out agent that, in the correct proportions, results in the formation of two immiscible aqueous phases. The incorporation of ILs in ABS for metal extraction has the potential to increase tunability, decrease the viscosity associated with ILs and reduce the necessary quantity of IL.[12] However, most ABS are not stable at low pH values,[13] which is a key requirement to prevent metal hydrolysis and precipitation. To address this issue acidic aqueous biphasic systems (AcABS) have recently been proposed.[14] In AcABS, the salts conventionally used as salting-out agents

63 are replaced by an acid which acts as a salting-out agent and simultaneously enables the leaching

64 and stability of metals. Typically, the phase with the highest acid weight percentage (wt %) is

65 named as acid-rich phase and the one with the highest IL wt % is referred to as IL-rich phase.

66 Similarly to ABS, AcABS can feature a thermoresponsive behavior, namely lower critical solution

67 temperature (LCST).[15,16] The potential thermoresponsive character of AcABS provides another

68 degree of freedom to adjust the metal extraction performance.

69 The novelty of AcABS and the ionic nature of ILs can be a challenge for the identification of

70 possible metal extraction mechanisms in these systems.[17,18] Typically, metal cations are highly

71 hydrated causing them to have an affinity to the acid-rich phase and low extraction to the IL-rich

72 phase. For metal extraction to be successful it is important to promote the formation of more

73 hydrophobic metal complexes.[19] Although this is often accomplished by adding extractants, in

74 AcABS the IL simultaneously acts as a phase-forming agent and extractant.[14] Similarly to other

75 liquid-liquid extraction systems, several metal extraction mechanisms can occur in AcABS with

76 unfunctionalized ILs, such as anion-exchange or ion-pair extraction.[5,19] The anion-exchange

77 mechanism is a metathesis reaction in which the transfer of the negatively charged metal-

78 complex to the IL-rich phase is dependent on the migration of the IL anion to the acid-rich

79 phase.[5] The ion-pair extraction mechanism occurs when the metal speciation in the aqueous

80 and IL-rich phase differ such that the IL forms a hydrophobic ion pair with the aqueous metal

81 complex to promote its partition. The hydrophobic ion-pair can be formed using cations present

82 in the acid phase or in the IL-rich phase. It is important to note that the final extracted metal ions

83 by unfunctionalized ILs are often present as anionic complexes in the IL-rich phase regardless of

84 the extraction mechanism.

85   Several AcABS were shown to extract and separate transition metals and rare earth elements.

86 [14,20,21] Despite their promising efficiency, the influence of the IL anion and acid on the

87 mechanisms of extraction of metals in AcABS remain poorly studied particularly for systems in

88 which the IL and acid anions are not identical (split-anion extraction).[22] To address the gaps in

89 this field, herein we develop AcABS based on hydrophilic ILs (tributyltetradecylphosphonium

90 chloride, $[P_{44414}]Cl$, and tributyltetradecylphosphonium sulfate, $[P_{44414}][HSO_4]$) and biphasic

91 systems based on the hydrophobic IL tributyltetradecylphosphonium nitrate, $[P_{44414}][NO_3]$ for the

92 extraction of four transition metals – Cu(II), Co(II), Ni(II) and Mn(II) – and a rare-earth metal,

93 Ce(IV). To evaluate the influence of the acid in the extraction of different metals, hydrochloric,

94 sulfuric and nitric acid were used to form the different biphasic systems. The thermoresponsive

95 character of the systems was also explored and metal partition was evaluated at 298 K and 323

96 K.

2. Experimental section

2.1. Materials

99 The ILs [P_{44414}]Cl (> 95 wt %), [P_{44414}][HSO_4] (> 95 wt %) and [P_{44414}][NO_3] (> 95 wt %) were

100 purchased from Iolitec and used as received. The inorganic acids HCl (37 wt %) and H_2SO_4 (95 wt

101 %) were obtained from Fisher Scientific and HNO_3 (65 wt %) was obtained from Chem-Lab.

102 $CoCl_2 \cdot 6H_2O$ (> 99 wt %), $CoSO_4 \cdot 7H_2O$ (> 99 wt %), $Co(NO_3)_2 \cdot 6H_2O$ (> 99 wt %), $CuSO_4 \cdot 5H_2O$ (> 99

103 wt %), $Cu(NO_3)_2 \cdot 3H_2O$ (>99.5 wt %), $MnCl_2 \cdot 4H_2O$ (> 99 wt %) and $Ni(NO_3)_2 \cdot 6H_2O$ (> 99 wt %) were

104 obtained from Merck. $CuCl_2 \cdot 2H_2O$ (> 98 wt %) and $NiCl_2 \cdot 6H_2O$ (> 98 wt %) were purchased from

105 Analar. $NiSO_4 \cdot 6H_2O$ (> 99 wt %) and $Mn(NO_3)_2 \cdot 4H_2O$ (> 96 wt %) were purchased from Riedel de

106 Haen. $Ce(SO_4)_2 \cdot 4H_2O$ (> 98 wt %) and $MnSO_4 \cdot 4H_2O$ (> 99 wt %) were obtained from Alfa Aesar

107 and Panreac, respectively. The deionized water was obtained through a Millipore filter system

108 MilliQ®. Yttrium standard (1000 mg·L^{-1} of Y(III) in 2 % nitric acid) was purchased from Sigma

109 Aldrich.

2.2. Acidic aqueous biphasic systems

111 The use of [P_{44414}]Cl to form an AcABS with HCl (298 K and 323 K), H_2SO_4 (298 K) and HNO_3

112 (298 K) as salting-out agents was previously reported.[23] The remaining ternary phase diagrams

113 presented in this work – [P_{44414}]Cl-H_2SO_4-H_2O (323 K), [P_{44414}][HSO_4]-HCl-H_2O (298 K and 323 K),

114 [P_{44414}][HSO_4]-H_2SO_4-H_2O (298 K and 323 K) – were determined using the cloud point titration

115 method.[24,25] Temperature was controlled using a thermostatic bath ME-18 V Visco-

116 Thermostat Julabo and a temperature-controlled cell at 298.0 K or 323.0 K (± 0.1 K), atmospheric

117 pressure and continuous stirring. The binodal curves were determined by adding an acid aqueous

118 solution dropwise to a known amount of IL until the mixture becomes cloudy. At this point, water

119 is added dropwise until the mixture becomes clear. This procedure was alternately repeated as

120   many times as necessary. The composition of the ternary systems was determined via weight

121   quantification ($\pm$ 10^{-4} g) upon the addition of all components. Details related to the

122   determination of the phase diagrams, namely the experimental weight fraction data, can be

123   consulted in Table S1 and S2.

124   The mixture points used for metal extraction were selected considering the phase diagrams

125   in mol of solute (IL or acid) per kg of solvent (water + acid or water + IL, respectively). More details

126   are given in the Supporting Information. The IL concentration was set constant for all systems

127   and equal to 0.85 mol·kg^{-1}. Depending on the binodal curve, different acid concentrations were

128   used, as shown in Table 1. Mass fraction was calculated considering the total mass of the system

129   (water + acid + IL). The water content of the system was considered as the sum of the added

130   water plus the inherent water present in the acid solution (63 wt % for HCl, 35 wt % for HNO_3

131   and 5 wt % for H_2SO_4).

132   **Table 1.** Extraction mixture points in mol·kg^{-1} and wt %, with mixture point 1 ([Acid]$_1$) having a

133   lower acid content than mixture point 2 ([Acid]$_2$).

Biphasic system	Extraction points (mol·kg^{-1})			Extraction points (wt %)		
	[IL]	[Acid]$_1$	[Acid]$_2$	[IL]	[Acid]$_1$	[Acid]$_2$
[P$_{44414}$]Cl + HCl	0.85	6.5	8.0	27	19	23
[P$_{44414}$][HSO$_4$] + HCl	0.85	6.5	8.0	30	19	23
[P$_{44414}$][HSO$_4$] + H$_2$SO$_4$	0.85	2.5	4.0	30	20	28
[P$_{44414}$]Cl + H$_2$SO$_4$	0.85	3.0	4.0	27	22	28
[P$_{44414}$]Cl + HNO$_3$	0.85	2.5	4.0	27	14	20
[P$_{44414}$][NO$_3$] + HNO$_3$	0.85	2.5	4.0	28	14	20

134

135   To evaluate the effect of temperature on metal extraction, assays were carried out at (298 $\pm$

136   1) K and (323 $\pm$ 1) K. All solutions and mixture points were prepared gravimetrically by weighting

137   the correct amount of each component ($\pm$ 10^{-4} g). The mixture points were stirred and left to

138   equilibrate at (298 $\pm$ 1) K for at least 3 h, followed by centrifugation at 10 000 rpm for 2 min. The

139   extractions carried out at (323 $\pm$ 1) K were performed following a slightly different procedure.

140   Mixture points were prepared gravimetrically, stirred, and left to equilibrate at (323 $\pm$ 1) K. After

141 1 h, each mixture point was stirred again and the phases were left to separate overnight. In all

142 cases, the mass ($\pm$ 10^{-4} g) and volume ($\pm$ 5 $\times$ 10^{-3} mL) of each phase after separation were

143 registered.

144 **2.3. Metal solution preparation**

145 A multi-elemental stock solution (Co(II), Cu(II), Mn(II) and Ni(II)) was prepared with a

146 concentration of 0.2 mol·L^{-1} of each metal ion and diluted in the biphasic systems to yield a final

147 concentration of 0.01 mol·L^{-1}. To minimize the number of species present in each system, the

148 anion of the metal salt was selected to match the anion of the acid. Yet, $Ce(SO_4)_2$ was used as

149 Ce(IV) source in all ternary systems independently of the used acid. Due to the limited solubility

150 of Ce(IV) in certain systems, its partition was studied individually by preparing an aqueous

151 solution at 2 $\times$ 10^{-3} mol·L^{-1} of Ce(IV) in 37 wt % HCl, 50 wt % H_2SO_4 or 65 wt % HNO_3, the final

152 concentration of Ce(IV) being 1 $\times$ 10^{-3} mol·L^{-1} in each system.

153 **2.4. Instrumentation and measurements**

154 **2.4.1. Metal quantification**

155 The quantification of metal in each phase of the system was done using the total reflection

156 X-ray fluorescence spectrometer using a Picofox S2 (Bruker Nano (Billerica, MA, USA)) equipped

157 with a molybdenum X-ray source. The analysis was conducted at a 50 kV voltage and 600 µA

158 current. The quartz glass carriers were previously coated with 10 µL of silicon in isopropanol

159 solution and dried at (323 $\pm$ 1) K. Samples from each phase were diluted in polyvinyl alcohol (1

160 wt %) and spiked with a known concentration of yttrium. Of this solution, 10 µL were transferred

161 to a pre-treated quartz carrier and dried under high vacuum for at least 30 min. This procedure

162 was not applied for the top phase of the HNO_3-based systems since they are hydrophobic. For

163 this reason, the metal quantification in the top phase of these systems was accomplished by mass

164 balance from measurements of the acid-rich phase.

165 The distribution coefficient (*D*) was calculated as shown in Equation 1:

166
$$D = \frac{[M]_T}{[M]_B} \tag{1}$$

167 where $[M]_T$ is the metal concentration in the IL-rich top phase and $[M]_B$ is the metal concentration

168 in the bottom phase of the system. The extraction efficiency percentage (*EE* %) of each mixture

169 point was calculated according to Equation 2:

170
$$EE\ \% = \frac{m_T}{m_{Total}} \times 100 \qquad (2)$$

171 where m_T is the mass of metal in the top phase and m_{Total} is the total mass of metal in the system.

172 The separation factor (*Sf*) of the system was calculated according to Equation 3:

173
$$Sf = \frac{D_{M1}}{D_{M2}} \qquad (3)$$

174 where D_{M1} is the distribution coefficient of the most extracted metal and D_{M2} is the distribution

175 coefficient of the second most extracted metal to the top phase.

176   **2.4.2. In-phase water quantification**

177 To better understand the H_2O:HCl ratio in the top phase of the system composed of 27 wt % of

178 [P_{44414}]Cl and 23 wt % of HCl at various temperatures ((298, 313 and 323) K ± 1 K), the water

179 content of the top phase of this system was measured by coulometric Karl Fischer titration

180 (Metrohm, model 831). All measurements were performed in triplicates.

181   **2.4.3. Dynamic light scattering**

182 Dynamic Light Scattering (DLS) measurements (Malvern Zetasizer Nano-ZS) were performed on

183 the [P_{44414}]Cl-H_2SO_4-H_2O system spiked with 5 wt % of HCl to study the correlation between the

184 IL aggregate size and temperature. Briefly, samples were exposed to red light (HeNe laser, 565

185 nm) and the intensity variations of the scattered light were detected at a backscattering angle of

186 173°. The autocorrelation function was cumulatively analyzed by DTS v 7.03, which yielded the

187 aggregate size and the distribution. To complement this study, the type of Co(II) complexes

188 present in one of the systems was evaluated using a UV–Vis Synergy HT microplate reader from

189 BioTek at different temperatures.

190   **2.4.4. Ion-exchange evaluation**

191 The possibility of ion-exchange on the [P_{44414}]Cl-H_2SO_4-H_2O at 3.0 mol·kg^{-1} or 4.0 mol·kg^{-1} of

192 H_2SO_4 and on the [P_{44414}][HSO_4]-HCl-H_2O systems at 6.0 mol·kg^{-1} or 8.0 mol·kg^{-1} of HCl was

193   evaluated in the biphasic region by selecting a mixture point with 0.85 mol·kg^{-1} of IL. The mixtures

194   were agitated and left to equilibrate at (298 ± 1) K overnight. The two phases were separated

195   and weighed. The [P$_{44414}$]$^+$ was quantified by ^{1}H NMR. Chloride and hydrogen were quantified via

196   chloride ion-selective electrode (Metrohm) and titration, respectively.

3. Results and discussion

198   Aiming to better understand the effect of the IL anion and the acid on the partition of Cu(II),

199   Co(II), Ce(IV), Ni(II) and Mn(II), the following ternary systems were prepared:

200   [P$_{44414}$]Cl/[P$_{44414}$][HSO$_4$]-HCl-H$_2$O, [P$_{44414}$]Cl/[P$_{44414}$][HSO$_4$]-H$_2$SO$_4$-H$_2$O and [P$_{44414}$]Cl/[P$_{44414}$][NO$_3$]-

201   HNO$_3$-H$_2$O (*cf.* Table 1). Unlike [P$_{44414}$]Cl for instance, [P$_{44414}$][NO$_3$] is hardly miscible in water, and

202   can therefore be considered hydrophobic. For this reason, the [P$_{44414}$][NO$_3$]-HNO$_3$-H$_2$O system is

203   not an AcABS, but was studied for comparative purposes. Since the evaluated AcABS are

204   reversible temperature-induced systems with an LCST behavior, the effect of temperature on

205   metal partition was also evaluated at 298 K and 323 K (± 1 K). Transition metals Cu(II), Co(II), Ni(II)

206   and Mn(II) were studied in multi-elemental assays. The effect of the initial transition metal

207   concentration within the ternary systems was evaluated in the [P$_{44414}$]Cl-HCl-H$_2$O system and

208   details can be consulted in the Supporting Information Table S3 with no change in behavior

209   observed. Ce(IV) was studied in mono-elemental assays and only in the nitrate and chloride

210   systems due to its solubility limitations in systems containing [HSO$_4$]$^-$. All distribution coefficients

211   and extraction efficiencies presented are listed in the Supporting Information.

3.1. Metal distribution on [P$_{44414}$]Cl/[P$_{44414}$][HSO$_4$]-HCl-H$_2$O systems

213   Ion-exchange in the [P$_{44414}$][HSO$_4$]-HCl-H$_2$O system at 6.5 and 8.0 mol·kg^{-1} of acid was

214   evaluated by ^{1}H NMR, chloride ion-selective electrode and titration. The [P$_{44414}$]$^+$ cation is

215   quantitatively in the top phase. Chloride and hydrogen were similarly quantified in the bottom

216   phase at 6.5 mol·kg^{-1} (55 % Cl$^-$ vs 58 % H$^+$ of ions total amount in the system) and 8.0 mol·kg^{-1} of

217   HCl (69 % Cl$^-$ vs 73 % H$^+$) (see Table S4). Therefore, no significant ion-exchange was detected in

218   the [P$_{44414}$][HSO$_4$]-HCl-H$_2$O system. The binodal curves of all systems evaluated and mixture

219   points for metal extraction are represented in Figure S1 in the Supporting Information. The

220   influence of the IL anion (Cl$^-$ vs [HSO$_4$]$^-$) and acid content (HCl) on the extraction of the transition

221   metals Co(II), Cu(II), Ni(II), and Mn(II) and the lanthanide Ce(IV) were evaluated at 298 K with the

222   results presented in Figure 1.

223
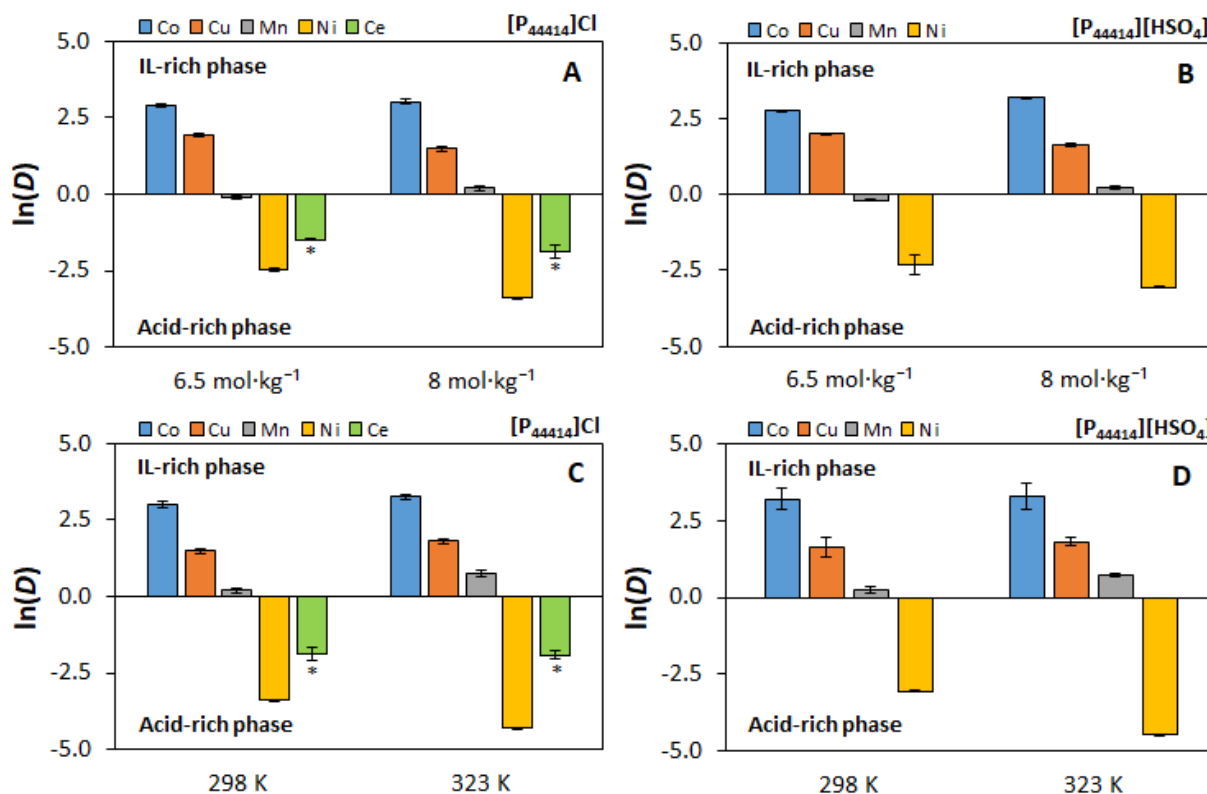
Figure 1. Effect of HCl concentration at (298 ± 1) K (A and B) and of temperature on metal distribution coefficient (D) in AcABS with 8.0 mol·kg^{-1} of HCl (C and D). The asterisk above Ce(IV) bars indicates that this element was studied in a mono-elemental assay.

227   Regardless of the HCl concentration, the distribution coefficient of metals increases in both

228   AcABS in the following way: Ni(II) < Ce(IV) < Mn(II) < Cu(II) < Co (II). The divergent distribution of

229   Co(II) and Ni(II) was also demonstrated when the [P$_{44414}$]Cl-HCl-H$_2$O system was first reported

230   [14] whilst Deferm *et al.* [26] reported a similar metal distribution ratio tendency (Ni(II) < Mn(II)

231   < Cu(II)) in the equivalent hydrophobic systems with the ILs [P$_{66614}$]Cl and [N$_{1888}$]Cl. The IL anion

232   (Cl$^-$ vs [HSO$_4$]$^-$) had a small influence on the distribution of metals considering the large excess of

233   Cl$^-$ provided by the acid (consult Table S5). Nevertheless, increasing the HCl concentration from

234   6.5 to 8.0 mol·kg^{-1} improved the distribution partition of Co(II) and Mn(II) and decreased the

235   distribution partition of Cu(II) and Ce(IV). This led to the enhancement of the $Sf_{Co(II)/Cu(II)}$ in the

236   AcABS based on [P$_{44414}$]Cl and [P$_{44414}$][HSO$_4$] from 2.6 to 4.6 and 2.1 to 4.8, respectively, at 6.5 to

237   8.0 mol·kg^{-1}. Despite the improvement of the distribution coefficients – excluding Cu(II) and

238   Ce(IV) – increasing the acid concentration did not impact the extraction efficiency values (see

239   Table S6). This is probably linked to the volume reduction of the IL-rich phase from 0.94 to 0.85

240   mL and 0.95 to 0.82 mL for [P$_{44414}$]Cl and [P$_{44414}$][HSO$_4$], respectively, when the HCl content

241   increases from 6.5 to 8.0 mol·kg^{-1}.

242   Extracted metal ions by unfunctionalized quaternary phosphonium or ammonium ILs

243   primarily exist as anionic complexes with the stability of the extracted metallic complex in the IL-

244   rich phase being typically independent of the acid-rich phase composition. However, this must

245   not be confused with the extraction efficiency which is strongly dependent on the overall system

246   composition. As such, the relative difference in the distribution ratio between the two species is

247   assigned to the dominant complex in the acid-rich phase, which is manipulated by the ionic

248   strength and complexing anion concentration in the solution. In Cl-rich systems, the distribution

249   ratio of each metal is related to their ability to form chloro-complexes and their respective

250   stability and affinity to the IL-rich phase.[14,17] This occurs through the displacements of water

251   molecules from the inner-sphere of the metal cation by chloride anions and the associated

252   change in the complex geometry in the case of Cu(II) and Co(II), and to a lesser extent Mn(II),

253   from octahedral to tetrahedral with the change in speciation.[17,27,28] A second less intuitive

254   contribution is the charge density of the resulting chloro-complexes and its influence on the

255   differing $D_{Co(II)}$ and $D_{Cu(II)}$ values given that the Co(II) and Cu(II) complexes identified in 6.5 mol·kg^{-1}

256   HCl by UV-vis are the positive [CoCl(H$_2$O)$_5$]$^+$ and anionic [CuCl$_4$]$^{2-}$ complexes respectively (Figure

257   S2).The Gibbs free energy of hydration (ΔG_{Hyd}°) for a given ionic complex is related to its charge

258   (z) and volume (V$_m$) by $\Delta G_{Hyd}^{\circ} \propto z^2/V_m^{1/3}$,[29] with smaller absolute ΔG_{Hyd}° values associated

259   with increased extraction.[30] As such, the [CoCl(H$_2$O)$_5$]$^+$ specie is expected to present a greater

260   distribution to the IL phase through an ion-pair mechanism compared to the [CuCl$_4$]$^{2-}$ anion

261   which occurs via anion-exchange. The low extraction of Ni(II) can be explained by its inability to

262   form fully dehydrated chloro-complexes under the studied conditions, preventing the formation

263   of hydrophobic interactions with the IL cation and, consequently, disabling its extraction towards

264   the IL-rich phase.[14,27] Poor Ni(II) extraction in chloride rich media was also reported by Zante

265 *et al.*[31] In the mentioned study, supported ionic liquid ($[P_{66614}][Cl]$) membranes afforded great

266 extraction of Co(II) over Ni(II), being this more evident at higher HCl concentrations.In the

267 $[P_{44414}]Cl$-HCl-H_2O system*,* higher temperatures result in higher distribution coefficients of the

268 studied metals (except Ni(II) and Ce(IV)) towards the IL-rich phase. The same trend was observed

269 in the $[P_{44414}][HSO_4]$-HCl-H_2O system, although to a lower extent. Increasing temperature caused

270 changes in the phase ratio and composition. At higher temperatures, the top phase shrinks,

271 leading to generally higher partition coefficient values. To better understand this phenomenon,

272 the H^+ content on each phase of the $[P_{44414}]Cl$-HCl-H_2O system with 8.0 mol·kg^{-1} of HCl was

273 evaluated by titration at 298 K, 313 K and 323 K (see Table S7). By considering all IL is in the top

274 phase it was possible to determine the water and acid content in each phase. The Cl/H_2O molar

275 ratio at 298 K, 313 K and 323 K is as follows: 0.26, 0.33 and 0.38. Therefore, as temperature

276 increases water is expelled from the IL-rich phase to the acid-rich phase, translating into a

277 decreased distribution of complexes with inner-sphere water molecules such as Ni(II) and Ce(IV).

278 **3.2. Metal distribution on $[P_{44414}]Cl$/$[P_{44414}][HSO_4]$-H_2SO_4-H_2O systems**

279 Ion-exchange in the $[P_{44414}]Cl$-H_2SO_4-H_2O system at 3.0 and 4.0 mol·kg^{-1} of acid was evaluated

280 by ^1H NMR and a chloride ion-selective electrode (see Table S8). The $[P_{44414}]^+$ cation is partitioned

281 quantitively to the top phase without traces of its presence in the bottom phase. Concerning the

282 Cl^-, 53 % and 57 % of this anion were found at the bottom phase at 3.0 and 4.0 mol·kg^{-1} of H_2SO_4,

283 respectively, being a clear indicator that considerable ion-exchange occurs in the $[P_{44414}]Cl$-

284 H_2SO_4-H_2O system. This is in agreement with results reported by Mogilireddy *et al.*[23]

285 Similar to the study performed for the HCl-based systems, the effect of the IL anion, acid

286 concentration and temperature were evaluated for the AcABS based on H_2SO_4. Due to the low

287 solubility of Ce(IV) in sulfate-rich systems, this metal was not evaluated in these AcABS. The

288 obtained results for the transition metals (Co(II), Cu(II), Mn(II) and Ni(II)) are represented in Figure

289 2. The differing biphasic region area of the $[P_{44414}]Cl$-H_2SO_4-H_2O and $[P_{44414}][HSO_4]$-H_2SO_4-H_2O

290 systems (see Figure S1) prevented the use of the same acid concentration for the mixture point

291 with lower acid content. At 2.5 mol·kg^{-1} of acid the $[P_{44414}]Cl$-H_2SO_4-H_2O system is in the

292 monophasic region. Thus, 3.0 mol·kg^{-1} of H_2SO_4 was considered as the lower acid content for this

293 system.

294
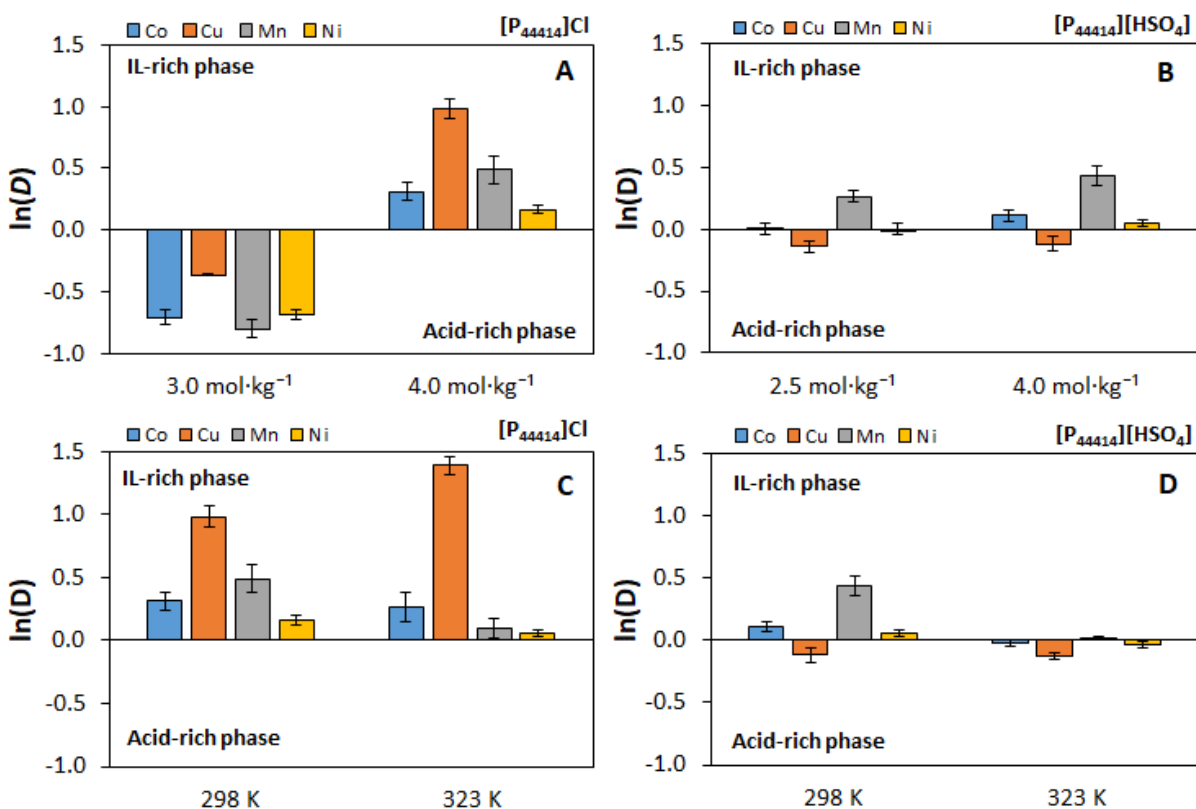
Figure 2. Effect of H_2SO_4 concentration at (298 ± 1) K (A and B) and of temperature on metal distribution (D) in AcABS containing 4.0 mol·kg^{-1} of H_2SO_4 (C and D).

Concerning the [P$_{44414}$]Cl system, at 3.0 mol·kg^{-1} of H_2SO_4 all metals partition preferentially to the acid-rich phase. Increasing the H_2SO_4 content to 4.0 mol·kg^{-1} increased the distribution of all metals to the IL-rich phase and changed the previously mentioned distribution coefficient trend to Ni(II) < Co(II) ≈ Mn(II) << Cu(II), with all metals showing a preference for the IL-rich phase. In the [P$_{44414}$][HSO$_4$] ternary system the metal distribution coefficient maintains the same tendency regardless of the acid concentration: Cu(II) < Ni(II) ≈ Co(II) < Mn(II). Similarly, Onghena *et al.*[32] reported that Co(II) extraction using a quaternary phosphonium IL increased with increasing H_2SO_4 concentration, attaining a maximum extraction at 11 mol·L^{-1} of H_2SO_4. The IL anion has a significant impact on the metal distribution behavior. The presence of Cl$^-$ from [P$_{44414}$]Cl promotes the extraction of Cu(II) to the IL-rich phase, especially at higher H_2SO_4 concentrations. The presence of different anions in the [P$_{44414}$]Cl-H_2SO_4-H_2O system enables the occurrence of a split anion extraction.[33] In this case, the metal ions are extracted from the acid-rich phase

13

310   containing $[HSO_4]^-/SO_4^{2-}$ anions to the IL-rich phase with Cl^- from the IL anion. Although the

311   formation of tetrahedral Cu(II)-chloride complexes is expected (as further confirmed and

312   discussed in sub-section 3.4.), the formation of mixed chloride-sulfate complexes may also be

313   possible. The formation of a metal-chloride complex with low charge density and thus lower

314   hydration enthalpy promotes the selective extraction of metals to the IL-rich phase. Charge

315   neutrality is maintained by restricted anion-exchange of the different anions between the two

316   phases. Higher H_2SO_4 concentrations translate into higher ionic strength within the AcABS which

317   improved the distribution ratio of Cu(II).

318   Increasing temperature was only relevant in the $[P_{44414}]Cl$ ternary system with Cu(II) having a

319   higher distribution coefficient and the remaining metals having a slightly lower distribution

320   coefficient to the top phase (Table S9). Despite the improvement in $D_{Cu(II)}$ with temperature (from

321   2.7 to 4.0), the extraction efficiency to the top phase remained very similar (73.4 to 74.7 %, *cf*.

322   Table S10). Once again, this is attributed to the phase ratio changes induced by temperature.

323   Increasing the temperature to 323 K resulted in the shrinkage of the top phase from 0.80 to 0.73

324   mL due to water expulsion as shown for the $[P_{44414}]Cl$-HCl-H_2O system (see Table S11).

325   Nevertheless, increasing temperature provided better selectivity values in the $[P_{44414}]Cl$ ternary

326   system (from $Sf_{Cu(II)/Mn(II)} = 1.6$ to $Sf_{Cu(II)/Mn(II)} = 3.6$). This feature enables the enhancement of the

327   separation factor of the AcABS without the need for additional acid or IL, making AcABS a

328   versatile and efficient alternative to other conventional solvent extraction techniques.

329   3.3. Metal distribution on $[P_{44414}]Cl/[P_{44414}][NO_3]$-$HNO_3$-$H_2O$ systems

330   The IL anion and acid concentration influence was evaluated for the systems composed of

331   HNO_3 at 3.0 and 4.0 mol·kg^{-1} with the distribution coefficients presented in Figure 3. In the

332   system composed of $[P_{44414}]Cl$ there is quantitative ion-exchange between the IL anion and

333   nitrate, leading to the formation of the hydrophobic IL $[P_{44414}][NO_3]$.[23] The hydrophobic

334   character of $[P_{44414}][NO_3]$ leads to the formation of a conventional liquid-liquid system, thus, the

335   designation AcABS is not applicable here.

336
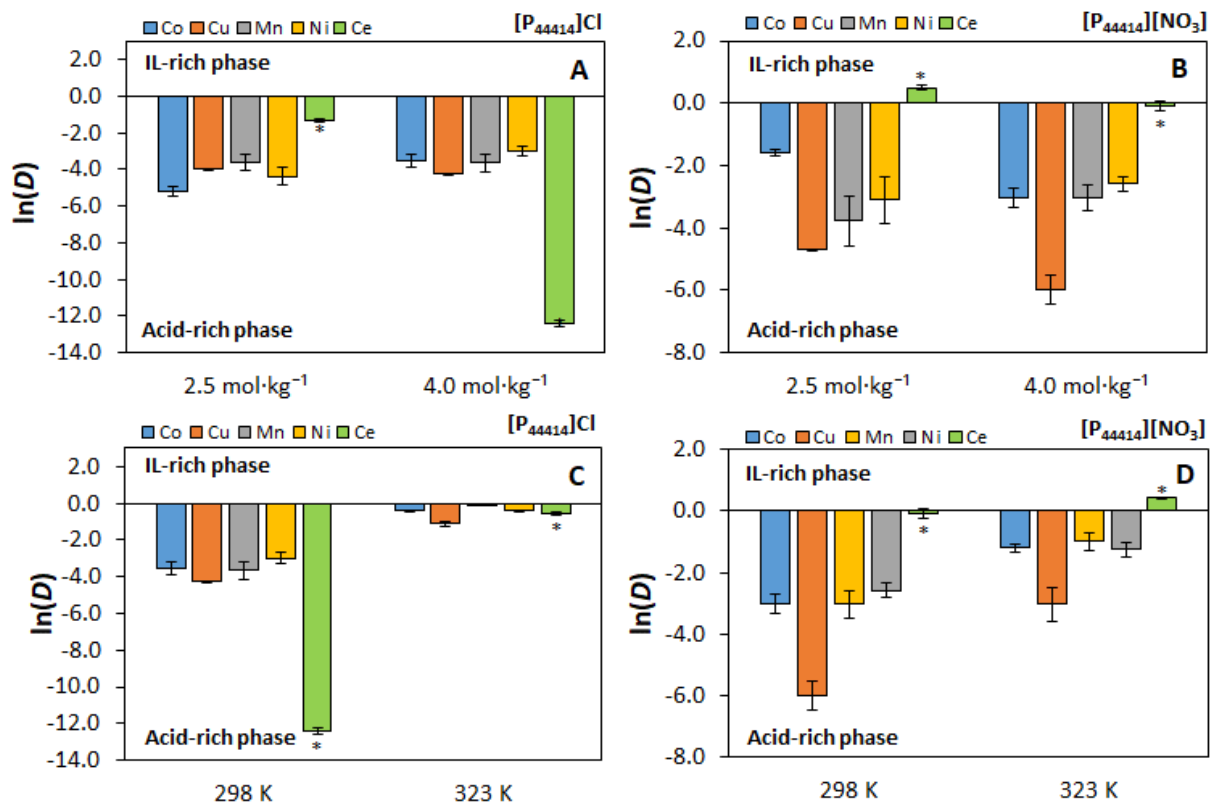
Figure 3. Effect of HNO_3 concentration at (298 ± 1) K (A and B) and of temperature on metal distribution (D) in the biphasic systems containing 4.0 mol·kg^{-1} of HNO_3 (C and D).

Regardless of the IL anion, Co(II), Cu(II), Mn(II) and Ni(II) display very low affinity for the IL-rich phase ($D \ll 1$). In contrast, Ce(IV) affinity for the IL-rich phase improved by changing the IL anion from Cl$^-$ to NO_3^- (Table S12 and S13). The favored distribution of Ce(IV) over transition metals to the IL-rich phase in AcABS composed of HNO_3 was also reported by Schaeffer *et al.*[20] The ternary system $[N_{4444}][NO_3]$ + HNO_3 + H_2O was shown to be selective for Ce(IV) against other trivalent lanthanides and transition metals. In this system, extraction was suggested to occur via ion-pair formation as the identified $[Ce(NO_3)_6]^{2-}$ complex in the IL-rich phase was absent in the acid-rich phase before extraction. A similar ion-pair mechanism is proposed herein. However, the distribution coefficient of Ce(IV) decreases as the HNO_3 concentration increases, which may be related to the HNO_3 accumulation in the IL-rich phase.[20]

15

351   Since lower acid concentrations seem to enhance the affinity of Ce(IV) to the IL-rich phase,

352   an additional assay was performed at 1.0 mol·kg^{-1} of HNO$_3$. The results obtained are presented

353   in Figure 4.
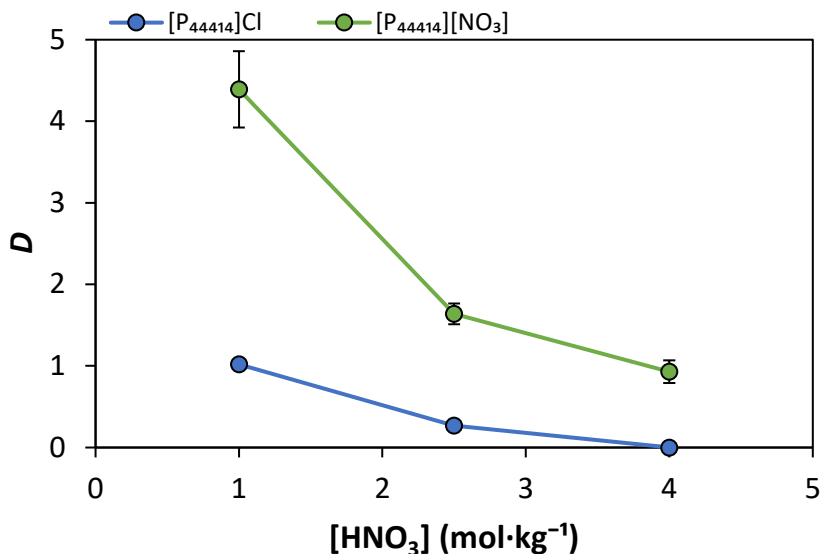
354

355   **Figure 4.** Metal distribution coefficient of the rare earth Ce(IV) on the [P$_{44414}$]Cl-HNO$_3$-H$_2$O (blue)

356   and [P$_{44414}$][NO$_3$]-HNO$_3$-H$_2$O (green) systems at 1.0, 2.5 and 4.0 mol·kg^{-1} of HNO$_3$ at (298 ± 1) K.

357

358   Reducing the acid concentration to 1.0 mol·kg^{-1} improved the extraction of Ce(IV) in both

359   systems. These results further support the hypothesis that nitric acid competes with metal ions

360   for the extractant (IL). Still, this does not seem to occur in other liquid-liquid extraction systems,

361   where increasing HNO$_3$ concentration affords better extraction efficiency values.[34]

362   Finally, increasing temperature results in higher values for metal distribution coefficients.

363   Still, the distribution coefficients values for all transition metals remain below 1, indicating a

364   better affinity for the acid-rich phase.

365   **3.4. Tuning AcABS extraction**

366   Results in the previous sections indicate that the primary factors influencing metal distribution

367   in AcABS can be summarized as listed below. These are meant to be used as general guidelines

368   based on systems studied here. However, it cannot be excluded that for certain AcABS-metal

369   pairings exceptions might occur.

370	(i)	Charge density of the metal complex. Metal complexes with lower charge density are
		more likely to partition to the IL-rich phase. This is affected by the presence of anions
		(A^-), coming either from the IL or the acid, liable to form the anionic complexes
		stabilized in the IL-rich phase. For example, Cu(II) extraction results in the [P$_{44414}$]Cl-
		HCl systems indicate that $D_{Cu(II)}$ decreases with increasing HCl concentration as the
		copper complex transitions from $CuCl_3^-$ to $CuCl_4^{2-}$ (Figure 1).

(ii) Absence of coordinated water molecules in the inner solvation sphere of the metal cation in the IL-rich phase. For example, Ni(II) presents a stable octahedral geometry across a wide range of chloride concentration, ensuring that even complexes of low charge density such as [NiCl·5H$_2$O]$^+$ and [NiCl$_2$·4H$_2$O] present a hydrophilic character and are therefore poorly extracted. Furthermore, whilst tetrahedral complexes of nickel are reported at elevated chloride concentrations and temperature ([NiCl$_2$(H$_2$O)$_2$] and [NiCl$_3$(H$_2$O)]$^-$), the fully chlorinated [NiCl$_4$]$^{2-}$ complex was not observed.[35]

(iii) n(A^-)/n(H$_2$O) ratio, keeping in mind that this ratio is significantly higher in the IL-rich phase after phase separation. The local n(A^-)/n(H$_2$O) ratio in the IL-rich phase can be modified through changes in the AcABS composition and temperature of the system.

(iv) Acid co-extraction, which can impair the extraction of the metal complexes to the IL-rich phase. In the systems studied, HNO$_3$ is a weaker acid than HCl and its protonated and dissociated form exist in equilibrium above 3.0 mol·L^{-1}, with the equilibrium likely shifted towards the protonated species in the IL-rich phase.[36] A similar reasoning applies in the case of sulfuric acid to the [HSO$_4$]$^-$↔SO$_4{}^{2-}$ pair.

Based on these findings, it is possible to tune the selectivity of the systems as exemplified below. In the [P$_{44414}$]Cl-H$_2$SO$_4$-H$_2$O system increasing H$_2$SO$_4$ concentration from 3.0 to 4.0 mol·kg^{-1} was found to cause significant changes in the distribution coefficient and the extraction efficiency of Cu(II), which improved from 0.70 to 2.67 and from 39 to 73 %, respectively (*cf.* Table S9 and S10 in the Supporting Information). Since H$_2$SO$_4$ is the acid most extensively used in the industry, the selectivity of the [P$_{44414}$]Cl-H$_2$SO$_4$-H$_2$O system is of interest. Aiming to take advantage of different acid selectivity, 1, 5 or 10 wt % of HCl was added to this system to improve Cu(II)

399 distribution. Values obtained for metal distribution coefficients and UV spectra of the top phases

400 of these systems are depicted in Figure 5 and further details can be found in Table S14.

401
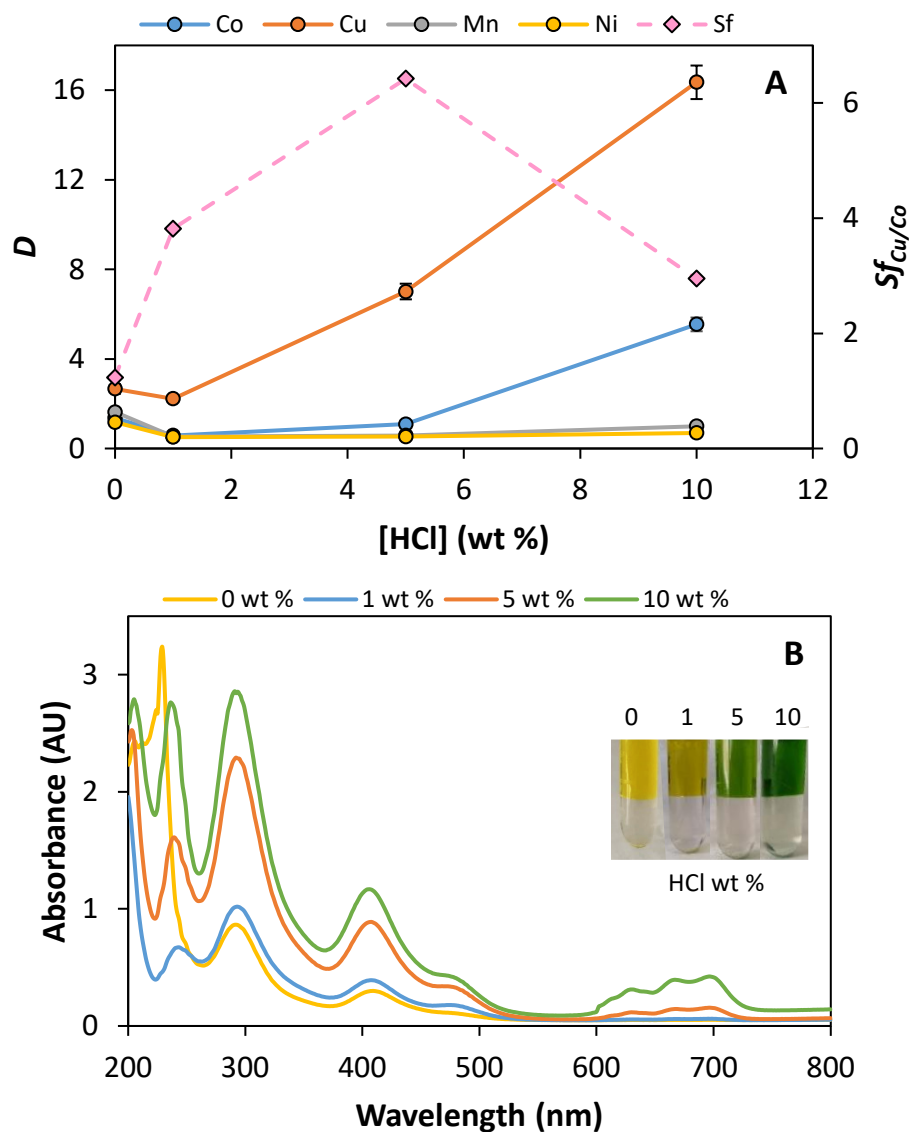
Figure 5. (A) Metal distribution coefficient (*D*) of different metals and separation factor (*Sf*) of
Cu(II) over Co(II) on the $[P_{44414}]Cl-H_2SO_4-H_2O$ system at 4.0 mol·kg^{-1} of H_2SO_4, and 0, 1, 5 or 10 wt
% of HCl at (298 ± 1) K. (B) UV spectra of the top phases of each $[P_{44414}]Cl-H_2SO_4-H_2O$ system
spiked with 0, 1, 5 or 10 wt % of HCl.

406 Addition of 1 wt % of HCl caused a small decrease in the extraction of Cu(II) to the top phase

407 and a significant decrease in the extraction of the remaining metals, causing the $Sf_{Cu(II)/Co(II)}$ to

408 improve from 1.2 to 3.8. Addition of higher amounts of HCl caused the formation of chloro-

409 complexes and a better distribution of Co(II) to the top phase. This is further confirmed by the
410 UV spectra of the top phases of these systems (Figure 5B). At 0 and 1 wt % HCl, no traces of
411 $[CoCl_4]^{2-}$ complexes are visible ($\approx$ 600 to 730 nm). However, increasing the HCl to 5 and 10 wt %
412 leads to the formation of cobalt-chloride complexes ($\approx$ 600 to 730 nm), followed by their
413 migration to the top phase resulting in higher distribution coefficients for Co(II). According to the
414 obtained UV spectra, copper-chloride complexes are present in the system regardless of the
415 addition of HCl ($\approx$ 250 to 500 nm). This shows that in this system, Cl$^-$ from the IL anion is sufficient
416 to form copper-chloride complexes, leading to their partition to the top phase. Regarding the
417 selectivity of the system, addition of 5 wt % HCl leads to a $Sf_{Cu(II)/Co(II)}$ = 6.4. However, increasing
418 the amount of added HCl to 10 wt % caused Co(II) to partition to a higher extent towards the top
419 phase, decreasing the $Sf_{Cu(II)/Co(II)}$ to 2.9. Adding 5 wt % of HCl provided the best selectivity, but
420 depending on the application, it may be profitable to simultaneously extract Co(II) and Cu(II) to
421 a higher extent by adding 10 wt % of HCl (EE_{Cu} % > 93 % and EE_{Co} % > 83 %, see Table S15). The
422 addition of small amounts of HCl to the $[P_{44414}]$Cl-H_2SO_4-H_2O system and the subsequent
423 formation of Cu(II)/Co(II)-chloro-complexes is a good way to promote system selectivity.
424 Although it is beyond the scope of this work, a similar behavior is anticipated if HCl is substituted
425 by chloride salts.

426   To gain a better understanding of the metal extraction mechanism of AcABS at ligand
427 concentrations below that for which anionic metal complexes are reported, the chloride deficient
428 $[P_{44414}]$Cl-H_2SO_4-H_2O system spiked with 5 wt % of HCl was further studied for the extraction of
429 Co(II). The system was prepared in the monophasic region by using 0.85 mol·kg^{-1} of $[P_{44414}]$Cl, 1.0
430 mol·kg^{-1} of H_2SO_4 and CoSO$_4$·7H$_2$O as a metal source. The type of cobalt-complexes and the IL
431 aggregate size were studied with temperatures ranging from 296 K to the appearance of the
432 biphasic regime at 313 K by UV–Vis and DLS, respectively. The obtained results are represented
433 in Figure 6. The same mixture was prepared with the same Cl$^-$ amount but without IL and
434 analyzed by UV–Vis for comparison purposes (see Figure S3).
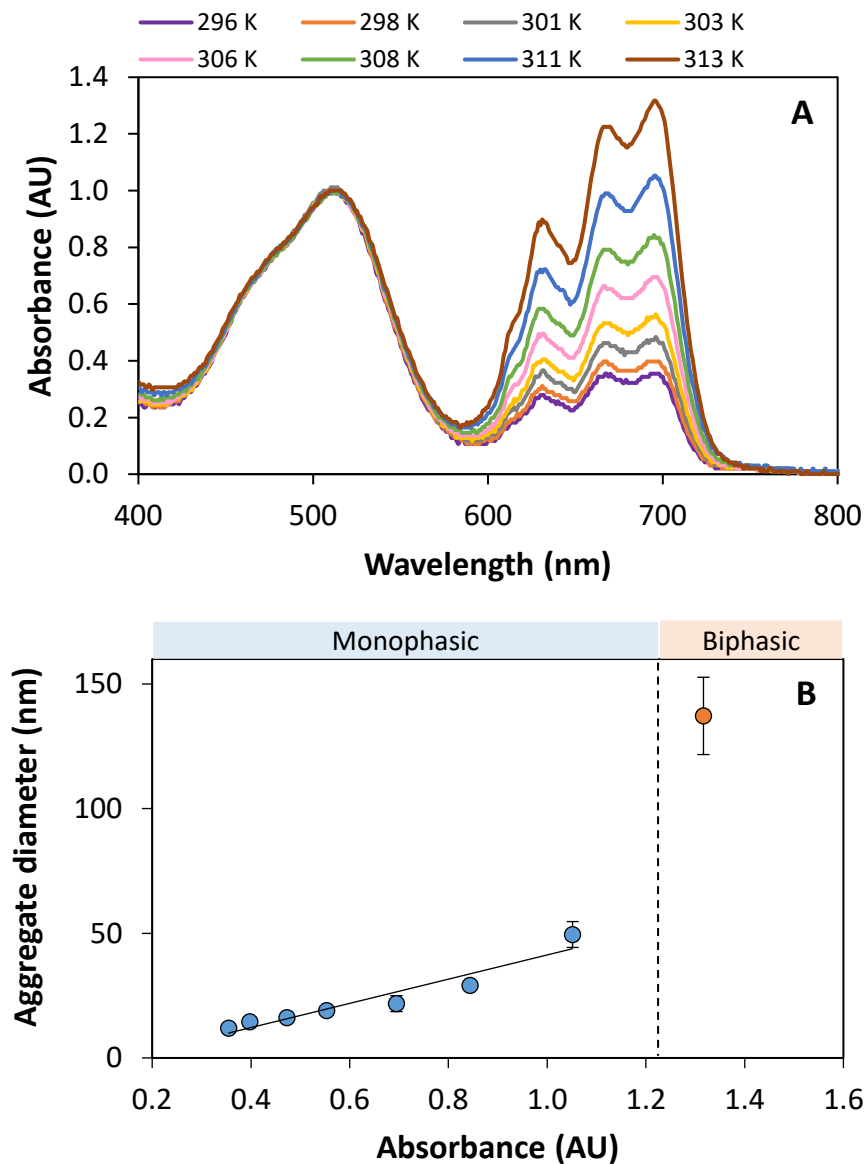
Figure 6. (A) UV–Vis spectrum of the $[P_{44414}]Cl$-H_2SO_4-H_2O mixture at 1.0 mol·kg^{-1} of H_2SO_4, 5 wt % of HCl and Co(II) as a metal source at different temperature values. The spectrum was taken at the monophasic region and standardized according to the peak at 514 nm. (B) Correlation between the average aggregate diameter present in the $[P_{44414}]Cl$-H_2SO_4-H_2O mixture and Co(II) relative absorbance at 695 nm (Abs = Abs695/Abs514) throughout the different evaluated temperature values.

At the lowest temperature values there is a high-intensity peak corresponding to Co^{2+} (514 nm) and a less intense peak corresponding to $CoCl_4^{2-}$ (695 nm). As the temperature increases and the system gets closer to the biphasic region, the peak intensity of $CoCl_4^{2-}$ increases. Recent SAXS

445   analysis on the [P$_{44414}$]Cl-HCl-H$_2$O system showed that the increase of both acid concentration

446   and/or temperature leads to micelle flocculation and is consistent with the presented DLS

447   analysis (Figure 6B).[16] Furthermore, increased [P$_{44414}$]Cl micelle counter-ion binding was

448   observed as the system approaches phase separation, resulting in the local accumulation of

449   chloride anion at the aggregate interface relative to the bulk concentration, thereby favoring the

450   interfacial formation of $CoCl_4^{2-}$. Moreover, in the absence of [P$_{44414}$]Cl, no $CoCl_4^{2-}$ is present in

451   the mixture regardless of the temperature (see Figure S3), reinforcing this interpretation.

452   Altogether, the obtained data suggest that the local increase in chloride anions through IL

453   aggregation induces the formation of $CoCl_4^{2-}$ even at low chloride concentration, suggesting an

454   ion-pair mechanism of extraction.

455   Overall, AcABS can be a promising alternative to conventional metal extraction techniques,

456   showing a good diversity of selectivities depending on the acid-IL conjugation, acid

457   concentration, temperature and target metal. The unalike distribution coefficient of the

458   transition metals and the rare earth studied herein also shows that AcABS could be a valuable

459   tool to separate lanthanides from transition metals. Besides the selectivity and versatility of

460   AcABS, these systems unlock the possibility to use the acid to simultaneously leach metals and

461   form the AcABS. This dual function of the acid is one of the main advantages of AcABS, enabling

462   to reduce the used amount of acid, the cost of the process and reducing the generated wastes.

463   In the case of split-anion extraction where significant anion-exchange occurs, care must be taken

464   during the stripping stage to regenerate the IL anion as this will otherwise affect the behavior of

465   the system over multiple extraction cycles.

4. Conclusion

467   Four AcABS and two hydrophobic liquid-liquid extraction systems were evaluated for the

468   separation of the transition metals Cu(II), Co(II), Ni(II) and Mn(II) and the rare earth Ce(IV). The

469   influence of the IL anion, acid and its concentration and temperature on metal distribution was

470   studied. The acid has a preponderant impact on metal distribution, the latter generally improving

471   as follows: HNO$_3$ < H$_2$SO$_4$ < HCl for transition metals and HCl < HNO$_3$ for Ce(IV). The temperature

472   affected the distribution of metals and the phase ratio within the biphasic systems. This was

473   attributed to the migration of water from the top to the bottom phase. The [P$_{44414}$]Cl-H$_2$SO$_4$-H$_2$O

afforded good Cu(II) selectivity which was further improved by the addition of 1 to 10 wt % of HCl. The best selectivity was achieved at 5 wt % of HCl ($Sf_{Cu(II)/Co(II)}$ = 6.4) and the metal extraction mechanism of this system was studied. The extraction of cobalt even at low chloride concentration was induced by the IL aggregation, highlighting the favorable nature of the ion-pair extraction mechanism and the versatile nature of AcABS. The versatility of AcABS makes them a promising alternative to conventional liquid-liquid extraction systems, with ILs having a dual role as phase forming agents and extractants. Altogether, this unlocks the possibility of simultaneous leaching and extraction of metals in a one-pot way.

Acknowledgments

Conflicts of interest: The authors declare no conflict of interest.

References

[1]   K.C. Sole, Solvent Extraction in the Hydrometallurgical and Purification of Metals: Process Design and Selected Applications, in: Solvent Extr. Liq. Membr., 1st ed., CRC Press, 2020: pp. 159–218. https://doi.org/10.1201/9781420014112-11.

[2]   T. Welton, Ionic liquids: a brief history, Biophys. Rev. 10 (2018) 691–706. https://doi.org/10.1007/S12551-018-0419-2/SCHEMES/3.

[3]   A.R.P. Gonçalves, X. Paredes, A.F. Cristino, F.J.V. Santos, C.S.G.P. Queirós, Ionic liquids—a

review of their toxicity to living organisms, Int. J. Mol. Sci. 22 (2021) 5612.
https://doi.org/10.3390/ijms22115612.

[4]   E.E. Tereshatov, V. Mazan, M. Boltoeva, C.M. Folden, Effect of hydrophobic ionic liquids
aqueous solubility on metal extraction from hydrochloric acid media: Mathematical
modelling and trivalent thallium behavior, Sep. Purif. Technol. 255 (2021) 117650.
https://doi.org/10.1016/j.seppur.2020.117650.

[5]   N. Schaeffer, H. Passos, I. Billard, N. Papaiconomou, J.A.P. Coutinho, Recovery of metals
from waste electrical and electronic equipment (WEEE) using unconventional solvents
based on ionic liquids, Crit. Rev. Environ. Sci. Technol. 48 (2018) 859–922.
https://doi.org/10.1080/10643389.2018.1477417.

[6]   J. Salminen, N. Papaiconomou, R.A. Kumar, J.M. Lee, J. Kerr, J. Newman, J.M. Prausnitz,
Physicochemical properties and toxicities of hydrophobic piperidinium and pyrrolidinium
ionic liquids, Fluid Phase Equilib. 261 (2007) 421–426.
https://doi.org/10.1016/j.fluid.2007.06.031.

[7]   M.G. Freire, P.J. Carvalho, R.L. Gardas, L.M.N.B.F. Santos, I.M. Marrucho, J.A.P. Coutinho,
Solubility of water in tetradecyltrihexylphosphonium-based ionic liquids, J. Chem. Eng.
Data. 53 (2008) 2378–2382. https://doi.org/10.1021/je8002805.

[8]   B. Onghena, T. Opsomer, K. Binnemans, Separation of cobalt and nickel using a
thermomorphic ionic-liquid-based aqueous biphasic system, Chem. Commun. 51 (2015)
15932–15935. https://doi.org/10.1039/c5cc06595j.

[9]   Y. Akama, M. Ito, S. Tanaka, Selective separation of cadmium from cobalt, copper, iron
(III) and zinc by water-based two-phase system of tetrabutylammonium bromide,
Talanta. 53 (2000) 645–650. https://doi.org/10.1016/S0039-9140(00)00555-5.

[10]   Y. Wang, S. Chen, R. Liu, L. Zhang, W. Xue, Y. Yang, Toward Green and Efficient Recycling
of Au(III), Pd(II) and Pt(IV) from Acidic Medium using UCST-Type Ionic Liquid, Sep. Purif.
Technol. (2022) 121620. https://doi.org/10.1016/J.SEPPUR.2022.121620.

[11]   N. Dubouis, C. Park, M. Deschamps, S. Abdelghani-Idrissi, M. Kanduc, A. Colin, M.

Salanne, J. Dzubiella, A. Grimaud, B. Rotenberg, Chasing Aqueous Biphasic Systems from Simple Salts by Exploring the LiTFSI/LiCl/H 2 O Phase Diagram, ACS Cent. Sci. 5 (2019) 640–643. https://doi.org/10.1021/acscentsci.8b00955.

[12]   L. McQueen, D. Lai, Ionic liquid aqueous two-phase systems from a pharmaceutical perspective, Front. Chem. 7 (2019) 135. https://doi.org/10.3389/fchem.2019.00135.

[13]   A.M. Ferreira, A.F.M. Cláudio, M. Válega, F.M.J. Domingues, A.J.D. Silvestre, R.D. Rogers, J.A.P. Coutinho, M.G. Freire, Switchable (pH-driven) aqueous biphasic systems formed by ionic liquids as integrated production-separation platforms, Green Chem. 19 (2017) 2768–2773. https://doi.org/10.1039/c7gc00157f.

[14]   M. Gras, N. Papaiconomou, N. Schaeffer, E. Chainet, F. Tedjar, J.A.P. Coutinho, I. Billard, Ionic-Liquid-Based Acidic Aqueous Biphasic Systems for Simultaneous Leaching and Extraction of Metallic Ions, Angew. Chemie. 130 (2018) 1579–1582. https://doi.org/10.1002/ange.201711068.

[15]   N. Schaeffer, G. Pérez-Sánchez, H. Passos, J.R.B. Gomes, N. Papaiconomou, J.A.P. Coutinho, Mechanisms of phase separation in temperature-responsive acidic aqueous biphasic systems, Phys. Chem. Chem. Phys. 21 (2019) 7462–7473. https://doi.org/10.1039/c8cp07750a.

[16]   G. Meyer, R. Schweins, T. Youngs, J.-F. Dufrêche, I. Billard, M. Plazanet, How temperature rise induces phase separation in acidic aqueous biphasic solutions, J. Phys. Chem. Lett. 13 (2022) 2731–2736. https://doi.org/10.1021/ACS.JPCLETT.2C00146.

[17]   R. Lommelen, T. Vander Hoogerstraete, B. Onghena, I. Billard, K. Binnemans, Model for Metal Extraction from Chloride Media with Basic Extractants: A Coordination Chemistry Approach, Inorg. Chem. 58 (2019) 12289–12301. https://doi.org/10.1021/acs.inorgchem.9b01782.

[18]   C.H.C. Janssen, N.A. Macías-Ruvalcaba, M. Aguilar-Martínez, M.N. Kobrak, Metal extraction to ionic liquids: the relationship between structure, mechanism and application, Int. Rev. Phys. Chem. 34 (2015) 591–622.

https://doi.org/10.1080/0144235X.2015.1088217.

[19]   P.D. Ola, M. Matsumoto, Metal Extraction with Ionic Liquids-Based Aqueous Two-Phase
        System, in: Recent Adv. Ion. Liq., IntechOpen, 2018.
        https://doi.org/10.5772/intechopen.77286.

[20]   N. Schaeffer, S.J.R. Vargas, H. Passos, P. Brandão, H.I.S. Nogueira, L. Svecova,
        Papaiconomou, J.A.P. Coutinho, A HNO3-Responsive Aqueous Biphasic System for Metal
        Separation: Application towards CeIV Recovery, ChemSusChem. 14 (2021) 3018–3026.
        https://doi.org/10.1002/cssc.202101149.

[21]   M.C. Hespanhol, B.M. Fontoura, J.C. Quintão, L.H.M. da Silva, Extraction and purification
        of gold from raw acidic electronic leachate using an aqueous biphasic system, J. Taiwan
        Inst. Chem. Eng. 115 (2020) 218–222. https://doi.org/10.1016/j.jtice.2020.10.027.

[22]   V.T. Nguyen, S. Rianõ, K. Binnemans, Separation of precious metals by split-anion
        extraction using water-saturated ionic liquids, Green Chem. 22 (2020) 8375–8388.
        https://doi.org/10.1039/d0gc02356f.

[23]   V. Mogilireddy, M. Gras, N. Schaeffer, H. Passos, L. Svecova, N. Papaiconomou, J.A.P.
        Coutinho, I. Billard, Understanding the fundamentals of acid-induced ionic liquid-based
        aqueous biphasic system, Phys. Chem. Chem. Phys. 20 (2018) 16477–16484.
        https://doi.org/10.1039/c8cp02862a.

[24]   C.M.S.S. Neves, S.P.M. Ventura, M.G. Freire, I.M. Marrucho, J.A.P. Coutinho, Evaluation
        of cation influence on the formation and extraction capability of ionic-liquid-based
        aqueous biphasic systems, J. Phys. Chem. B. 113 (2009) 5194–5199.
        https://doi.org/10.1021/jp900293v.

[25]   S.P.M. Ventura, S.G. Sousa, L.S. Serafim, Á.S. Lima, M.G. Freire, J.A.P. Coutinho, Ionic
        liquid based aqueous biphasic systems with controlled pH: The ionic liquid cation effect,
        J. Chem. Eng. Data. 56 (2011) 4253–4260. https://doi.org/10.1021/je200714h.

[26]   C. Deferm, M. Van De Voorde, J. Luyten, H. Oosterhof, J. Fransaer, K. Binnemans,
        Purification of indium by solvent extraction with undiluted ionic liquids, Green Chem. 18

(2016) 4116–4127. https://doi.org/10.1039/c6gc00586a.

[27]   Y. Marcus, Metal-chloride complexes studied by ion exchange and solvent extraction methods. II Transition-metal elements and the hexavalent actinides, Coord. Chem. Rev. 2 (1967) 257–297. https://doi.org/10.1016/s0010-8545(00)80125-3.

[28]   Z. Li, B. Onghena, X. Li, Z. Zhang, K. Binnemans, Enhancing Metal Separations Using Hydrophilic Ionic Liquids and Analogues as Complexing Agents in the More Polar Phase of Liquid-Liquid Extraction Systems, Ind. Eng. Chem. Res. 58 (2019) 15628–15636. https://doi.org/10.1021/acs.iecr.9b03472.

[29]   C.E. Housecroft, H.D. Brooke Jenkins, Absolute ion hydration enthalpies and the role of volume within hydration thermodynamics, RSC Adv. 7 (2017) 27881–27894. https://doi.org/10.1039/c6ra25804b.

[30]   D. Dupont, D. Depuydt, K. Binnemans, Overview of the effect of salts on biphasic ionic liquid/water solvent extraction systems: Anion exchange, mutual solubility, and thermomorphic properties, J. Phys. Chem. B. 119 (2015) 6747–6757. https://doi.org/10.1021/acs.jpcb.5b02980.

[31]   G. Zante, M. Boltoeva, A. Masmoudi, R. Barillon, D. Trébouet, Selective separation of cobalt and nickel using a stable supported ionic liquid membrane, Sep. Purif. Technol. 252 (2020) 117477. https://doi.org/10.1016/j.seppur.2020.117477.

[32]   B. Onghena, S. Valgaeren, T. Vander Hoogerstraete, K. Binnemans, Cobalt(II)/nickel(II) separation from sulfate media by solvent extraction with an undiluted quaternary phosphonium ionic liquid, RSC Adv. 7 (2017) 35992–35999. https://doi.org/10.1039/c7ra04753c.

[33]   K. Larsson, K. Binnemans, Separation of rare earths by split-anion extraction, Hydrometallurgy. 156 (2015) 206–214. https://doi.org/10.1016/j.hydromet.2015.04.020.

[34]   Y. Zuo, Y. Liu, J. Chen, Q. De Li, The separation of cerium(IV) from nitric acid solutions containing thorium(IV) and lanthanides (III) using pure [C8mim]PF6 as extracting phase, Ind. Eng. Chem. Res. 47 (2008) 2349–2355. https://doi.org/10.1021/ie071486w.

[35] Y. Tian, B. Etschmann, W. Liu, S. Borg, Y. Mei, D. Testemale, B. O'Neill, N. Rae, D.M. Sherman, Y. Ngothai, B. Johannessen, C. Glover, J. Brugger, Speciation of nickel (II) chloride complexes in hydrothermal fluids: In situ XAS study, Chem. Geol. 334 (2012) 345–363. https://doi.org/10.1016/j.chemgeo.2012.10.010.

[36] A. Ruas, P. Pochon, J.P. Simonin, P. Moisy, Nitric acid: Modeling osmotic coefficients and acid-base dissociation using the BIMSA theory, Dalt. Trans. 39 (2010) 10148–10153. https://doi.org/10.1039/c0dt00343c.